J Mater Sci (2008) 43:5489–5494
DOI 10.1007/s10853-008-2835-3

Physiochemical characterizations of nanobelts consisting of three mixed oxides (Co_3O_4, CuO, and MnO_2) prepared by electrospinning technique

Muzafar A. Kanjwal · Nasser A. M. Barakat · Faheem A. Sheikh · Myung Seob Khil · Hak Yong Kim

Received: 7 April 2008 / Accepted: 25 June 2008 / Published online: 16 July 2008

Abstract In this work, nanobelt mats consisting of three potential metal oxides have been produced using the electrospinning technique. An aqueous solution of cobalt acetate tetra-hydrate, copper acetate mono-hydrate, and manganese acetate tetra-hydrate was mixed with poly(vinyl alcohol) solution to prepare a sol–gel which was electrospun at 20 kV. The obtained nanofiber mats have been vacuously dried at 80 °C for 24 h and then calcined in air atmosphere at different temperatures and soaking times. The utilized physiochemical characterizations have affirmed that nanobelts composed of three oxides (Co_3O_4, CuO, and MnO_2) can be prepared by calcination at a temperature of 600 °C for 1 h. High-resolution transmission electron microscope and selected area electron pattern images revealed good crystallinity for the synthesized nanobelts.

M. A. Kanjwal
Department of Polymer Nano Science and Technology, Chonbuk National University, Jeonju 561-756, Republic of Korea

N. A. M. Barakat · F. A. Sheikh
Department of Bionano System Engineering, College of Engineering, Chonbuk National University, Jeonju 561-756, Republic of Korea

N. A. M. Barakat
e-mail: nasbarakat@yahoo.com

M. S. Khil · H. Y. Kim (✉)
Department of Textile Engineering, Chonbuk National University, Jeonju 561-756, Republic of Korea
e-mail: khy@chonbuk.ac.kr

Introduction

Metal oxides can adopt a large variety of structural geometries with an electronic structure that may exhibit metallic, semiconductor, or insulator characteristics, endowing them with diverse chemical and physical properties. Therefore, metal oxides are the most important functional materials using for chemical and biological sensing and transduction. Moreover, their unique and tunable physical properties have made themselves excellent candidates for electronic and optoelectronic applications. Nanostructured metal oxides have been actively studied due to both scientific interests and potential applications [1, 2]. One-dimensional (1D) nanomaterials including nanotubes, nanorods, nanowires, nanofibers, and nanobelts show some distinctive properties compared with other nanoparticles [3–5]. Among these 1D nanostructures, nanofibers and nanobelts do have especial interest due to high surface area to volume ratio. Many reports have been introduced to synthesis single oxide in the form of nanofibers or nanobelts. However, single oxides have limited electrochemical properties. In order to produce 1D nanostructure with novel chemical and physical properties, some researchers have turned on synthesizing nanostructure consisting of two oxides [6–13].

In this study, we report preparing nanobelts consisting of mixture of three functional oxides (Co_3O_4, CuO, and MnO_2). Co_3O_4-based materials are suitable candidates for the construction of solid-state sensors [14, 15], heterogeneous catalysts [16, 17], electrochromic devices [18], solar energy absorbers [19, 20]. Cupric oxide has been pointed out as a suitable compound for cathodes in lithium batteries [21]. Also, CuO is known as *p*-type semiconductors in general and hence potentially useful for constructing junction devices such as PN junction diodes [22]. Apart

from semiconductor applications, cupric oxide has been employed as heterogenous catalysts for several environmental processes [23, 24], solid-state gas sensor heterocontacts [25, 26] and microwave dielectric materials [27]. MnO_2 have been intensively investigated as promising electrode materials in primary/secondary batteries and electrochemical capacitors due to their excellent electrochemical performance, low-cost, nonpoisonous nature, environmental friendliness, and convenient preparation [28–30]. Furthermore, it can be used in the photovoltaic devices [31, 32]. Accordingly, the aim of the present study was combining these three oxides in single 1D nanostructure; we think this novel mixture will have distinct physical properties and will have good utilizing.

Smooth and incessant nanobelts of a mixture consisting of the aforementioned oxides have been prepared by electrospinning technique. Sol–gel precursor containing cobalt acetate tetrahydrate, copper acetate monohydrate, manganese acetate tetrahydrate, and poly(vinyl alcohol) (PVA) has been electrospun. The dried nanofiber mats were calcinied in air atmosphere at 600 °C for 1 h. The obtained material was analyzed by powder X-ray diffraction analysis (XRD), energy dispersive X-ray analysis (EDX), transmission electron microscopy (TEM), thermal gravimetric analysis (TGA), scanning electron microscopy (SEM), and Fourier transform infrared spectroscopy (FT-IR). The obtained results assured that final product is pure three mixed oxide nanobelts.

Experimental details

Materials

Manganese (II) acetate tetra hydrate (MnAc) 99.9 assay, copper (II) acetate mono hydrate (CuAc) 98.0 assay were obtained from Showa Co. Japan. Cobalt (II) acetate tetra hydrate (CoAc) 98.0 assay was purchased from Junsei Co. Ltd., Japan. PVA with a molecular weight (MW) = 65,000 g/mol obtained from Dong Yang Chem. Co., South Korea. These materials were used without any further purification. Distilled water was used as solvent.

Experimental work

An aqueous metal acetates solution was prepared by dissolving CoAc, MnAc, and CuAc in water with the ratio of 1:1:1:12. A sol–gel was prepared by mixing the obtained metal acetates solution with PVA aqueous solution (10 wt%) with a ratio of 7.5:20. Typically, 0.5 g from each metal acetate was dissolved in 6 g water, and then mixed with 20 g of PVA (10 wt%). The mixture was vigorously stirred at 50 °C for 5 h. The final solution obtained was placed in a plastic capillary. A copper pin connected to a high-voltage generator was inserted in the solution, and the solution was kept in the capillary by adjusting the inclination angle. A ground iron drum covered by polyethylene sheet was serving as a counter-electrode. A voltage of 20 kV was applied to the solution. The formed nanofiber mats were initially dried for 24 h at 80 °C under vacuum, and then calcined at 600 °C for 1 h in an air with a heating rate of 2 °C/min.

Characterization

Surface morphology was studied by JEOL JSM-5900 SEM, JEOL Ltd., Japan, and field-emission SEM (FE-SEM, Hitachi S-7400, Japan) equipped with energy dispersive X-ray (EDX). The phase and crystallinity were characterized by using Rigaku X-ray diffractometer (Rigaku Co., Japan) with Cu Kα (λ = 1.54056 Å) radiation over a range of 2θ angles from 10 to 100°. High-resolution image and selected area electron diffraction pattern were observed by JEOL JEM 2010 TEM operating at 200 kV (JEOL Ltd., Japan). Spectroscopic characterization has been investigated by FT-IR, the spectra were recorded as KBr pellets using Varian FTS 1000 FT-IR, Mid-IR spectral range, cooled DTGS detector, Scimitar series, Varian Inc., Australia. Thermal gravimetric has been achieved via Pyris1 TGA analyzer (PerkinElmer Inc., USA).

Results and discussion

Figure 1 shows the SEM images of metal acetates/PVA-dried nanofiber mats in low and high magnifications. As shown in Fig. 1b, mixing of more than one acetate metal does not affect the efficiency of the electrospinning process. In other words, electrospinning of the prepared sol–gel produced smooth and continuous nanofibers. Figure 2 shows the frequency curve of the prepared nanofibers. As shown in this figure, the metal acetates/PVA nanofibers diameters laid with a relatively narrow range. According to the data embedded in Fig. 2, the average diameter of these nanofibers is 375 nm. Calcination of the metal acetates/PVA nanofiber mats affected drastically on the nanofibrous morphology. Figure 3 shows the SEM micrographs of the obtained material. As can be observed from Fig. 3b which reveals a high-magnification SEM image, the nanofibers obtained due to the electrospinning process have been altered to nanobelts. The average diameter of these nanobelts can be estimated from the frequency of diameters curve as shown in Fig. 4. The obtained nanobelts do have an average diameter of 235 nm. Figure 5a and b reveals the FE-SEM image for the original metal acetate/PVA nanofiber before calcination and a single nanobelt obtained due

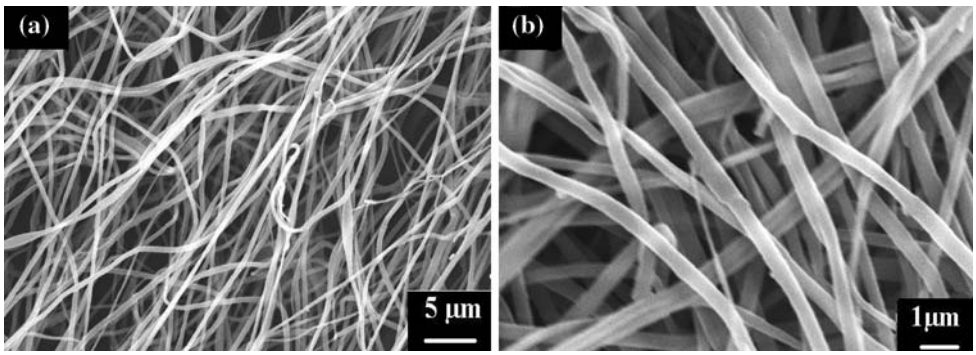

Fig. 1 SEM images for the original metal acetates/PVA nanofiber mats. (**a**) Low magnification and (**b**) high magnification

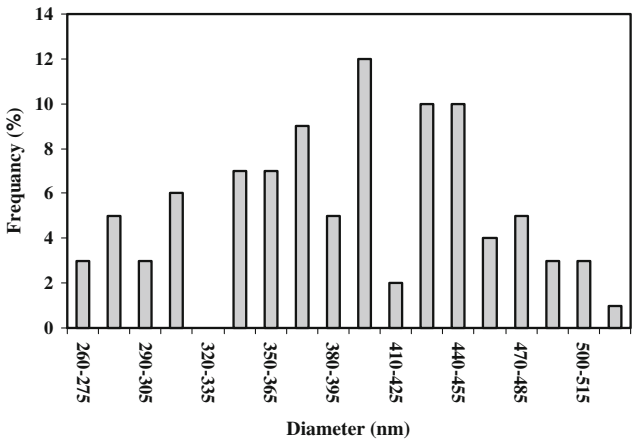

Fig. 2 Diameters frequency distribution curve for the metals acetates/PVA nanofiber mats

to calcination, respectively. As clearly shown in Fig. 5b, the cross section of the obtained material is not circular, it is irregular shape, although the electrospinning technique produced nanofibers with almost circular cross section as shown in Fig. 5a. Therefore, we can say that calcination of the metal acetate/PVA nanofiber mats at 600 °C has converted the 1D shape from nanofiber to nanobelt.

It is noteworthy mentioning that the ceramic materials in general and metal oxides in particular tend to sinter at high temperature. Sintering of these materials always accompanies by size diminishing. According to this phenomenon, we can explain formation of nanobelts from nano-fibrous form as a sintering of two adjacent nanofibers especially the obtained nanobelts do have the dumbbell shape as can be observed from Fig. 5b. Low nanofibers density and high polymer content in the original mat enhanced agglomeration of only two nanofibers at the mentioned calcination temperature and holding time. Changing the calcination temperature or the soaking time produced nanoparticles rather than nanofibers or nanobelts as was indicated from many achieved experiments (data not shown). The particle size was small at calcination temperatures lower than 600 °C, however, big size was observed at high temperatures which indicates agglomeration of many nanofibers. Figure 6 shows an illustration for the mechanism of formation of nanobelt from two nanofibers.

According to thermal properties of PVA and the acetate anion, one can say that calcination of the prepared nanofiber mats at such used temperature completely eliminated PVA and decomposed the metal acetate into inorganic metal compounds. The typical XRD pattern of produced material is presented in Fig. 7. As shown in this figure, the standard peaks of the cobalt (II, III) oxide (Co_3O_4), copper (II) oxide (CuO), and manganese dioxide (MnO_2) are

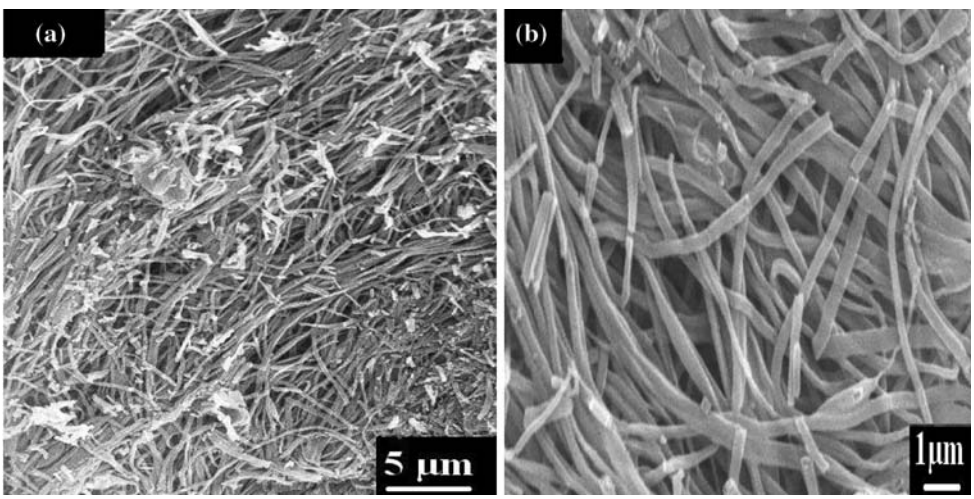

Fig. 3 Low (**a**) and high (**b**) magnifications of SEM micrographs for the nanofibers obtained after calcination at 600 °C for 1 h

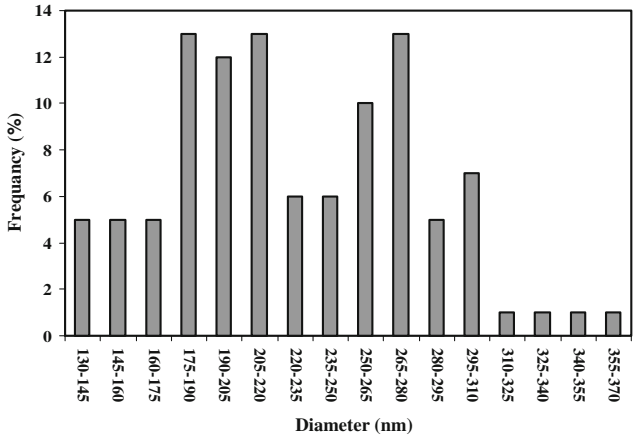

Fig. 4 Diameters frequency distribution curve for nanofibers obtained after the calcination process

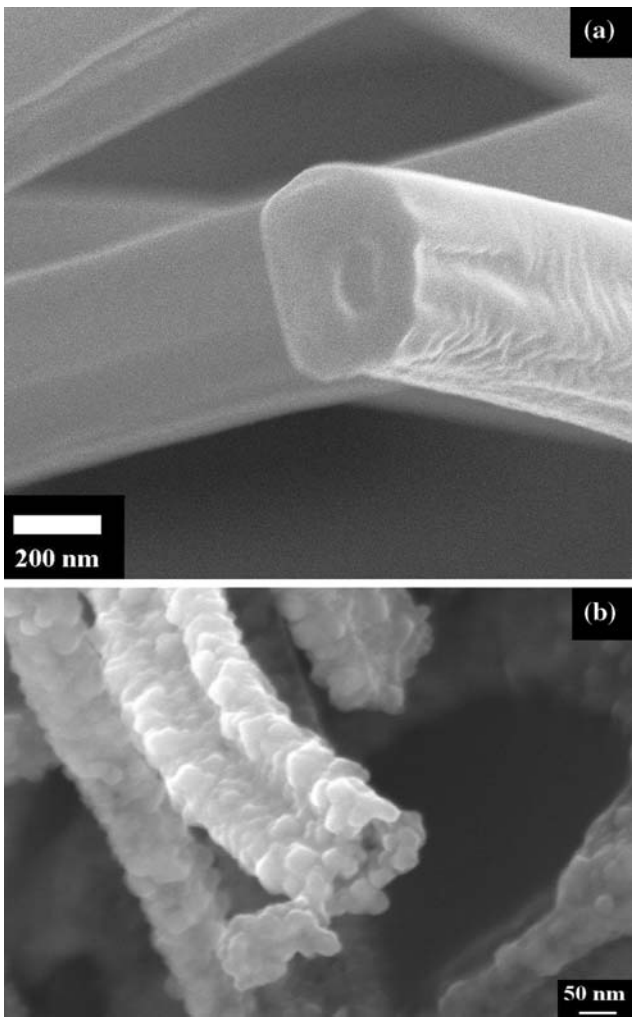

Fig. 5 FE-SEM micrograph showing the cross-sectional shape of the metal acetates/PVA electrospun nanofibers (**a**), and the obtained nanobelts after the calcination process (**b**)

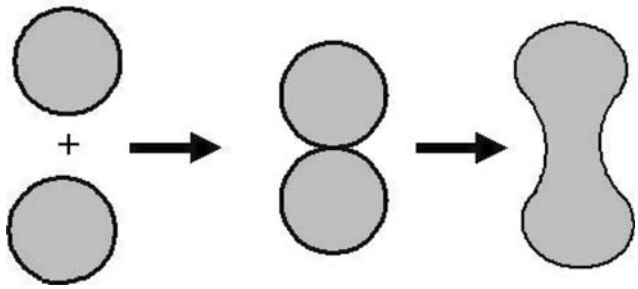

Fig. 6 Illustration for the mechanism of forming nanobelt from two adjacent nanofibers

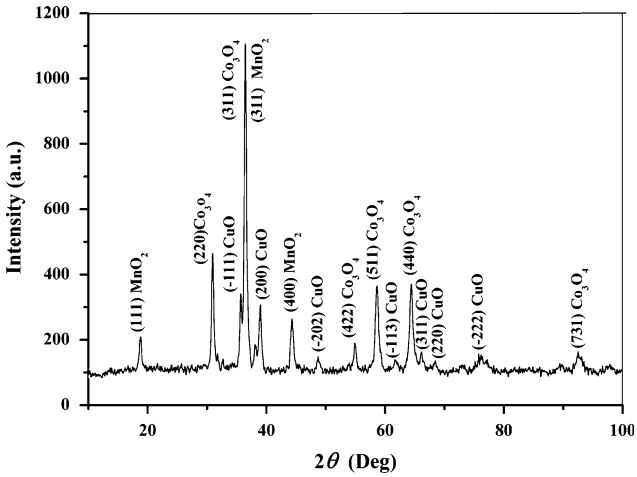

Fig. 7 XRD results for the prepared nanobelts after calcination process

observed. The existence of strong diffraction peaks at 2θ values of 36.8, 59.2, 65.2, and 28.6° corresponding to (311), (511), (440), and (220) indicating the formation of Co_3O_4 [JCDPS card no. 42-1467]. However, the peaks appeared at 2θ of 35.4, 38.8, and 61.7° corresponding to the crystal planes of (−111), (200), and (−113) affirmed formation of CuO [JCDPS card no. 05-0661]. Also, some peaks were noticed at 19.1, 36.8, and 45.2° which denote crystal planes of (111), (311), and (400), respectively; these peaks can be invoked to confirm synthesizing of MnO_2 [JCDPS card no. 42-1169]. All the appeared peaks have been identified as shown in Fig. 7.

In order to confirm the results obtained from the XRD, EDX analysis (equipped with FE-SEM instrument) has been invoked. With taken metals as a base, the molar ratio of Co:Cu:Mn:O in a mixture consisting of Co_3O_4, CuO, MnO_2 would be 1:1:1:13/3. Therefore, the theoretical atomic percentages of Co, Cu, Mn, and O have to be 13.64, 13.64, 13.64, and 59.08%, respectively. A close real result has been obtained from EDX analysis as shown in Fig. 8. This result supports the XRD data and simultaneously confirms formation of the aforementioned oxides.

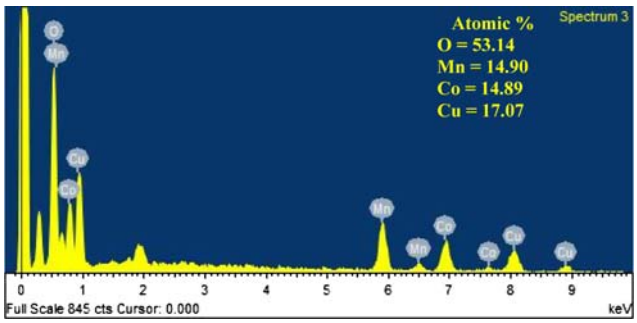

Fig. 8 EDX results for the obtained nanobelts, the inset reveals the element atomic percentages

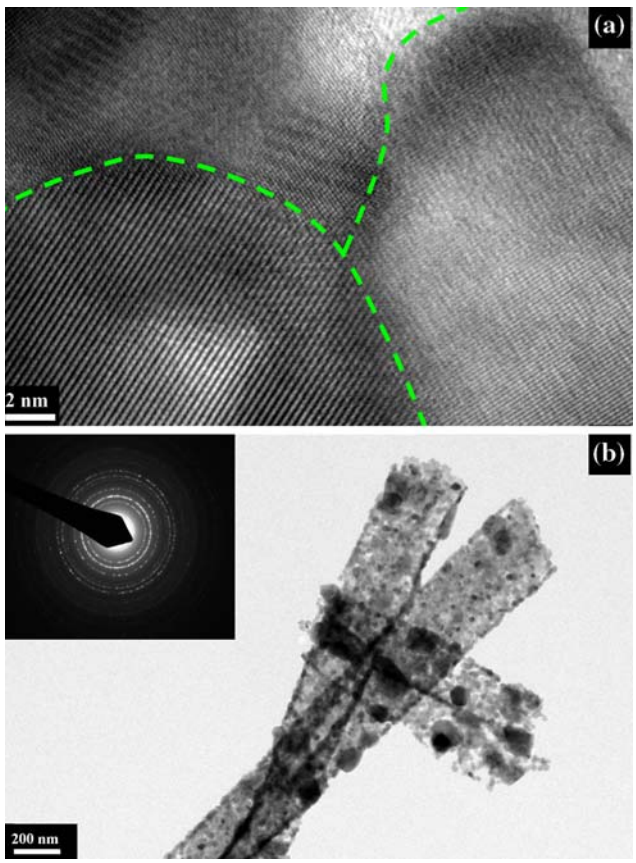

Fig. 9 (**a**) HRTEM micrograph for the nanobelts obtained after the calcination process. (**b**) TEM image showing the nanobelts and selected area electron pattern diffraction (inset)

Figure 9 shows the high-resolution TEM image of the calcined nanofibers and the TEM image. As shown in Fig. 9a the atomic planes uniformly arrange in parallel way which indicates good crystallinity. Moreover, three types of crystal planes with different distances between the successive planes can be observed in the figure which refers to the three oxides. Figure 9b shows TEM images of some nanobelts. This figure considerably affirms formation of separate nanobelts. The inset in Fig. 9b shows the SAED

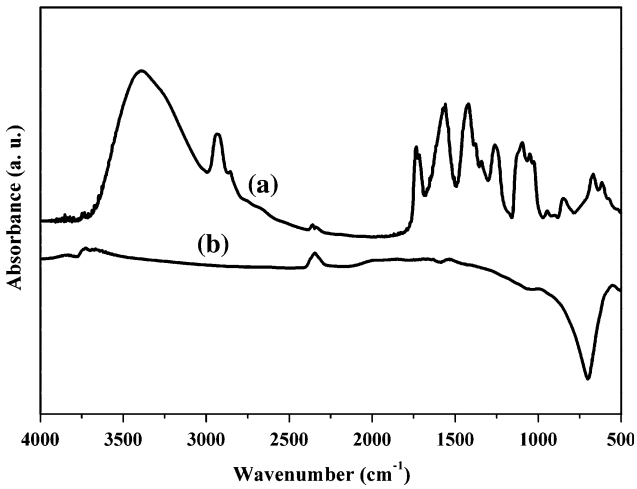

Fig. 10 FT-IR results for the metals acetates/PVA mats before (a) and after (b) the calcination process

pattern, there are no dislocations or imperfections observed in the lattice planes which confirm good crystallinity of the synthesized nanobelts.

FT-IR is an analytical technique being widely utilized to investigate the chemical bonds. Figure 10 shows the IR spectra for the metal acetates/PVA nanofiber mats and the produced nanobelts. In the metal acetates/PVA spectra, there are characteristic absorption bands of CO^{-2} at 1,568 and 1,417 cm^{-1}, as well as those of C–C bonds at 1,250 cm^{-1}. Moreover, the spectrum shows a broadband centered at around 3,332 cm^{-1} as well as weak bands at 846, 934, 1,028, and 1,093 cm^{-1}. These bands are attributed to stretching, wagging, and twisting vibrations of the water of hydration [33]. Also, the peak at 1,735 cm^{-1} represents H_2O absorbed by the nanofibers [34]. The characteristics absorption bands of the acetate anion appear from 1,590 to 600 cm^{-1} [35]. As can be seen in this figure, the various peaks revealing to PVA and acetate anion cannot be observed in the spectra of the produced nanobelts.

Figure 11 shows the TGA data, the first derivative has been plotted in the same figure to get more precise information. As shown in the first derivative curve, there are two distinct peaks appear at ~220 and 240 °C. The first peak is denoting to the elimination of PVA [36], so, the only explanation of the second one is decomposition of the acetates anions; especially there is no other noteworthy peaks in the curve. Moreover, Fig. 11 indicates that the metal oxides are completely synthesized at a temperature of 360 °C since there is no weight change after this temperature. Actually, many experiments have been conducted to get good morphology at relatively low temperature; however, we got nanobelts at 600 °C only, discrete and agglomerated nanoparticles were obtained at lower and higher temperatures than the utilized one, respectively.

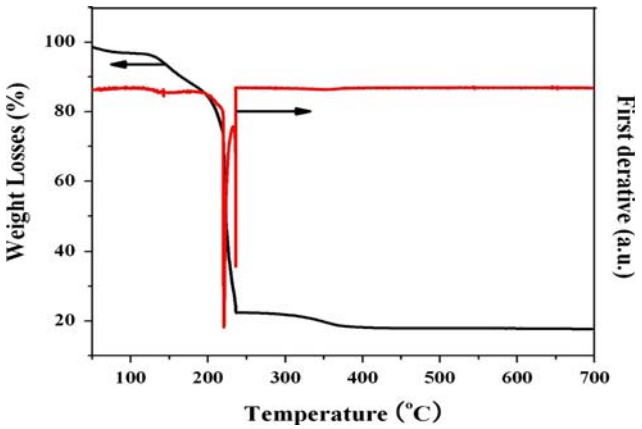

Fig. 11 TGA and the corresponding first derivative results for the metal acetates/PVA mats in oxygen atmosphere

Conclusion

Calcination of the nanofiber mats produced by electrospinning of a sol–gel consisting of cobalt acetate tetrahydrate, copper acetate monohydrate, manganese acetate tetrahydrate, and PVA in air atmosphere at 600 °C for 1 h completely eliminates the PVA polymer and decomposes the metal acetates into Co_3O_4, CuO, and MnO_2. According to the wide applications of the used oxides and the advantage of nanobelts shape, the obtained mixed nanobelts might have good utilization in heterogenous catalysis, lithium-ion batteries electrodes, solar energy absorbers, and other applications.

Acknowledgement This work was supported by Korean Research Foundation Grant founded by Korean Government (MOEHRD). (The Center for Health Care Technology, Chonbuk National University, Jeonju 561-756, Republic of Korea.)

References

1. Cavicchi RE, Silsbe RH (1984) Phys Rev Lett 52:1435. doi:10.1103/PhysRevLett.52.1453
2. Ball P, Li G (1992) Nature 355(6363):761. doi:10.1038/355761a0
3. Lieber CM (2003) MRS Bull 28(7):486
4. Xia YN, Yang PD (2003) Adv Mater 15(5):351. doi:10.1002/adma.200390086
5. Sander MS, Prieto AL, Gronsky R, Sands T, Stacy AM (2002) Adv Mater 14(9):665. doi:10.1002/1521-4095(20020503)14:9<665::AID-ADMA665>3.0.CO;2-B
6. Dai HQ, Gong J, Kim HY, Lee D (2002) Nanotechnology 13(5):674. doi:10.1088/0957-4484/13/5/327
7. Dharmaraj N, Kim CK, Prabu P, Ding B, Kim HY, Viswanathamurthi P (2007) Int J Electrospun Nanofibers Appl 1(1):63
8. Yuh JH, Nino JC, Sigmund WM (2005) Mater Lett 59(28):3645. doi:10.1016/j.matlet.2005.07.008
9. Ju YW, Park JH, Jung HR, Choa SJ, Lee WJ (2008) Mater Sci Eng B 147(1):7. doi:10.1016/j.mseb.2007.10.018
10. Peng XS, Meng GW, Wang XF, Wang YW, Zhang J, Liu X et al (2002) Chem Mater 14(11):4490. doi:10.1021/cm025567o
11. Zhou XF, Zhao Y, Cao X, Xue YF, Xu DP, Jiang L et al (2008) Mater Lett 62(3):470. doi:10.1016/j.matlet.2007.05.063
12. Shaoa CL, Yua N, Liu YC, Mu RX (2006) J Phys Chem Solids 67(7):1423. doi:10.1016/j.jpcs.2006.01.104
13. Yu N, Shao CL, Liu YC, Guan HY, Yang XH (2005) J Colloid Interface Sci 285(1):163. doi:10.1016/j.jcis.2004.11.014
14. Yamaura H, Tamaki J, Moriya K, Miura N, Yamazoe N (1997) J Electrochem Soc 144(6):L158. doi:10.1149/1.1837710
15. Ando M, Kobayashi T, Lijima S, Haruta M (1997) J Mater Chem 7(9):1779. doi:10.1039/a700125h
16. Nkeng P, Koening J, Gautier J, Chartier P, Poillerat G (1996) J Electroanal Chem 402(1–2):81. doi:10.1016/0022-0728(95)04254-7
17. Weichel S, Moller P (1998) J Surf Sci 399(2–3):219. doi:10.1016/S0039-6028(97)00820-0
18. Burke LD, Lyons ME, Murphy OJ (1982) J Electroanal Chem 132:247. doi:10.1016/0022-0728(82)85022-5
19. Hutchins MG, Wright PJ, Grebenik PD (1987) Sol Energy Mater 16(1–3):113. doi:10.1016/0165-1633(87)90013-X
20. Ramachandram K, Oriakhi CO, Lerner MM, Koch VR (1996) Mater Res Bull 31(7):767. doi:10.1016/0025-5408(96)00070-0
21. Podhajecky P, Scrosati B (1985) J Power Sources 16(4):309. doi:10.1016/0378-7753(85)80095-1
22. Muhibbullah M, Hakim MO, Choudhury MGM (2003) Thin Solid Films 423(1):103. doi:10.1016/S0040-6090(02)00970-7
23. Ortiz JR, Ogura T, Medina-Valtierra J, Acosta-Ortiz SE, Bosh P, de los Reyes JA et al (2001) Appl Surf Sci 174(3–4):177. doi:10.1016/S0169-4332(00)00822-9
24. Kharas KCC (1993) Appl Catal B Environ 2(2–3):207. doi:10.1016/0926-3373(93)80049-J
25. Vasiliev RB, Rumyantseva MN, Yakovlev NV, Gaskov AM (1998) Sens Actuators B Chem 50(3):186. doi:10.1016/S0925-4005(98)00235-4
26. Nakamura Y, Zhuang H, Kishimoto A, Okada O, Yanagida H (1998) J Electrochem Soc 145:632. doi:10.1149/1.1838315
27. Kim DW, Park B, Chung JH, Hong KS (2000) Jpn J Appl Phys 39(5A):2696. doi:10.1143/JJAP.39.2696
28. Reddy RN, Reddy RG (2004) J Power Sources 132(1–2):315. doi:10.1016/j.jpowsour.2003.12.054
29. Toupin M, Brousse T, Belanger D (2004) Chem Mater 16(16):3184. doi:10.1021/cm049649j
30. Subramanian V, Zhu H, Vajtai R, Ajayan PM, Wei B (2005) J Phys Chem B 109(43):20207. doi:10.1021/jp0543330
31. Chaudhary YS, Agrawal A, Shrivastav R, Satsangi VR, Dass S (2004) Int J Hydrogen Energy 29(2):131. doi:10.1016/S0360-3199(03)00109-5
32. Yoon KH, Choi WJ, Kang DH (2000) Thin Solid Films 372(1–2):250. doi:10.1016/S0040-6090(00)01058-0
33. Yamani Z, Buyers WJL, Cowley RA, Prabhakaran D (2008) Physica B 403(5–9):1406
34. Li T, Yang SG, Huang LS, Gu BX, Du YW (2004) Nanotechnology 15(11):1479. doi:10.1088/0957-4484/15/11/018
35. Jiang Y, Wu Y, Xie B, Xie Y, Qian YT (2002) Mater Chem Phys 74(2):234. doi:10.1016/S0254-0584(01)00463-1
36. Afzal M, Butt PK, Ahrnad H (1991) J Therm Anal 37(5):1015. doi:10.1007/BF01932799